UDK 691.714.018.8:621.794.4
Original scientific article/Izvirni znanstveni članek

ISSN 1580-2949
MTAEC9, 56(5)507(2022)

# STUDY ON DESCALING CHARACTERISTICS OF 304 STAINLESS STEEL USING PICKLING AND ABRASIVE WATER JET

## ŠTUDIJ ODSTRANJEVANJA OKSIDIRANE POVRŠINE Z NERJAVNEGA JEKLA VRSTE 304 Z JEDKANJEM IN ABRAZIVNIM CURKOM

**Jiawei Liu[1,*], Jingtao Han[1,2], Ruilong Lu[1]**

[1]University of Science and Technology Beijing, Haidian, Beijing, China
[2]Guangzhou Sino Precision Steel Tube Industry Research Institute, Zengcheng District, Guangzhou, China

*Prejem rokopisa – received: 2022-04-12; sprejem za objavo – accepted for publication: 2022-08-01*

doi:10.17222/mit.2022.474

The variability in the surface integrity, mechanical properties and corrosion resistance of the surface layer of 304 stainless steel after scale removal by pickling and an abrasive water jet, removing the oxide and Cr-poor layer was studied comparatively. It was found that the surfaces of the pickling specimens were etched with pits of varying sizes, with $R_a$ of 4.384 μm and $R_z$ of 24.81 μm, while the surface microhardness fluctuated in a range of 200–220 HV. The surfaces of the abrasive water jet specimens exhibited a stack laminar characteristic, $R_a$ of 3.960 μm and $R_z$ of 22.63 μm, while the surface microhardness decreased with an increase in the distance from the surface; the surface microhardness increased from the original 210 HV to 380–390 HV, producing a 1-mm deep work-hardening layer, which had a great impact on the microhardness of the substrate 0–0.3 mm from the surface. For both the pickling specimens and the abrasive water jet specimens, the material tensile strength and yield strength were slightly increased, and the elongation after fracture was significantly reduced. The corrosion resistance of the pickling specimens was better than that of the abrasive water jet specimens. The surface layer of the AWJ specimens generated a Cr-poor layer due to severe secondary oxidation, and the corrosion resistance of the material was reduced.

Keywords: 304 stainless steel, pickling, abrasive water jet, descaling

Avtorji opisujejo primerjalno študijo sprememb integritete površine, mehanskih lastnosti in odpornosti proti koroziji površinske plasti nerjavnega jekla vrste 304 po odstranitvi škaje (oksidirane površine) z dvema različnima postopkoma: jedkanjem in abrazivnim vodnim curkom za odstranitev oksidne in s kromom revne plasti. Ugotavljajo, da so med jedkanjem površine testnih vzorcev nastale jedkalne jamice različnih velikosti z $R_a$ 4,384 μm in z $R_z$ je 24,81 μm, mikrotrdota površine vzorcev pa je bila podobna izvorni in se je spreminjala od 200 HV do 220 HV. Površina testnih vzorcev obdelanih z abrazivnim vodnim curkom je imela stopničaste laminarne značilnosti z $R_a$ je 3,96 μm in $R_z$ je 22,63 μm, površinska mikrotrdota vzorcev pa se je zmanjševala s povečevanjem oddaljenosti šobe curka vode od površine in se je z izvornih 210 HV povišala na od 380 HV do 390 HV. Pri tem je nastala 1 mm globoka utrjena plast, ki je imela večji vpliv na mikrotrdoto podlage do globine 0,3 mm. V primerjavi z jedkanimi testnimi vzorci sta pri z vodnim curkom obdelanih vzorcih natezna trdnost in meja plastičnosti jekla rahlo narasli, medtem, ko je bil raztezek po zlomu pomembno nižji. Korozijska odpornost jedkanih vzorcev je bila boljša od vzorcev obdelanih z abrazivnim vodnim curkom. Površinska plast z abrazivnim vodnim curkom obdelanih vzorcev generira na kromu revno plast zaradi močne sekundarne oksidacije in tako je korozijska odpornost materiala zmanjšana.

Ključne besede: nerjavno jeklo vrste 304, jedkanje, abrazivni curek vode, odstranjevanje škaje

## 1 INTRODUCTION

The 304 stainless steel has excellent corrosion resistance, cold formability and weldability. It is widely used in food, medical and home decoration industries, nuclear and paper industries.[1–3] However, due to their chemical composition and austenitic microstructure, the low mechanical strength and poor wear resistance of austenitic stainless steels have become major obstacles to their application.[4] In addition, the oxide scale, burr and oil contamination, formed during the machining process, are also inconvenient for the subsequent operations such as welding and assembly.[5]

The use of $H_2SO_4$ as a pre-acid solution with $HNO_3$-HF mixed pickling is the internationally most widely used stainless-steel pickling process. The $HNO_3$-HF pickling process takes on the multiple pickling functions of removing the oxide layer, poor-Cr layer and passivating the substrate, which is prone to incomplete removal of the poor-Cr layer and severe local corrosion in an actual production.[6] Meanwhile, $NO_x$ is inevitably generated during a pickling process, which greatly increases the environmental pressure of stainless-steel enterprises due to the paroxysmal characteristics of $NO_x$. Li et al.[7] studied the hydrogen embrittlement phenomenon occurring in stainless steel and found that the hydrogen embrittlement mechanism of stainless steel mainly includes the hydrogen weak bond theory, hydrogen local plastic deformation theory and the synergistic effect between the two, while the hydrogen embrittlement caused by pickling leads to a reduction of the mechanical properties of stainless steel. The reduction of the mechanical properties of the material should not be ignored.

*Corresponding author's e-mail:
liu_jiawei163@163.com (Jiawei Liu)

**Table 1:** Chemical composition of 304 stainless steel (*w*/%)

| Element | C | Mn | P | S | Si | Cr | Ni | Fe |
|---|---|---|---|---|---|---|---|---|
| Average | 0.07 | 2.0 | 0.04 | 0.02 | 0.72 | 19.2 | 10.2 | balance |

Post-mixed high-pressure abrasive water jet (AWJ) is an environmental surface treatment technology. Reasonable process parameters can effectively remove the oxide and Cr-poor layer from the surface of stainless steel, while the formation of a nanocrystalline hardening layer and residual stress field on the surface can significantly improve the fatigue strength and wear resistance of the 304 stainless steel.[8] The size of the surface roughness after descaling is determined by the combination of jet pressure, abrasive and target material,[9] and a reasonable configuration of the three can obtain the target roughness value. The substrate is in an activated state after AWJ descaling and is prone to secondary oxidation in a wet environment. The problem of rapid passivation of the surface after AWJ descaling needs to be solved by research. Wang et al.[10] found that after shot peening, strain-induced martensite was generated on the surface layer of austenitic stainless steel. This phenomena also appeared during an AWJ process, and the effect of strain-induced martensite on the properties of the material should not be ignored.

Environmental pollution from the descaling of 304 stainless steel using pickling is a growing problem. With the development of the high-pressure technology, AWJ as a green and non-polluting descaling technology is receiving more and more attention from scholars. But there are few reports comparing the similarities and differences between the descaling effects of pickling and AWJ on 304 stainless steel. In this paper, pickling and AWJ were used to remove the oxide and Cr-poor layer from the surface of 304 stainless steel, and the variability in the surface integrity, mechanics properties and corrosion resistance after descaling were comparatively studied to provide a reliable basic research reference for the application of the abrasive water jetting technology in the descaling of 304 stainless steel.

## 2 EXPERIMENTAL PART

The experimental material was a 304 stainless steel (06Cr19Ni10) wire ($\phi$ 6.5 mm) and its chemical composition is shown in **Table 1**.

### *2.1 Pickling*

The original specimen was the 304 stainless steel wire of $\phi$ 6.5 mm × 150 mm. A 205g/L $H_2SO_4$ solution was heated to 60 °C in a DK-98-1 electric thermostatic water bath. The original specimen was pickled for 30 min and then dried with a hot-air blower. The mixed acid solution (a concentration of 120 g/L of HF and 50 g/L of $H_2SO_4$ ) was heated to 40 °C; the specimen was pickled for 60 min, then taken out and dried with the hot-air blower to get a pickled specimen (referred to as the pickling specimen).

### *2.2 Abrasive water jet*

The experimental equipment was a self-developed stainless-steel wire acid-free descaling production line, using abrasive water jets to efficiently remove the oxide layer and Cr-poor layer from the surface of the stainless-steel wire, with automatic take-up and discharge functions. The equipment included 3 pairs of nozzles; the angle between the axes of each nozzle pair was 120° and the three-dimensional structure of the arrangement is shown in **Figure 1**. The nozzle-cavity structure parameters are shown in **Figure 2**. The experimental parameters included a jet pressure of 35 MPa, pulling speed of 12 m/min, target distance of 80 mm and injection angle of 80°. The abrasive material was a 304 stainless steel shot of $\phi$ 0.3 mm, the flow rate of the abrasive material was 8–10 kg/min, and the surface moisture was dried by hot air at the exit of the descaling box; a specimen of $\phi$ 6.5 mm × 150 mm was intercepted after the AWJ descaling (referred to as the AWJ specimen).

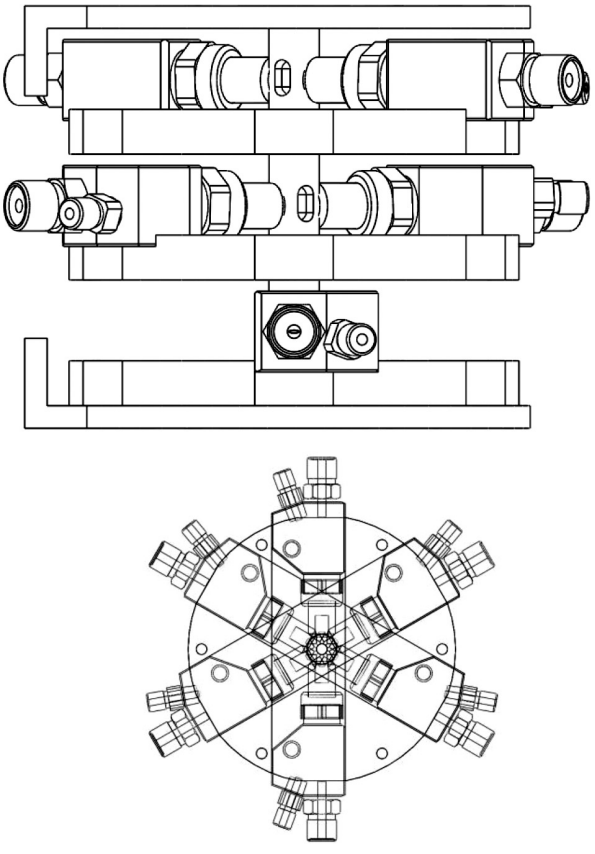

**Figure 1:** Layout of the nozzles

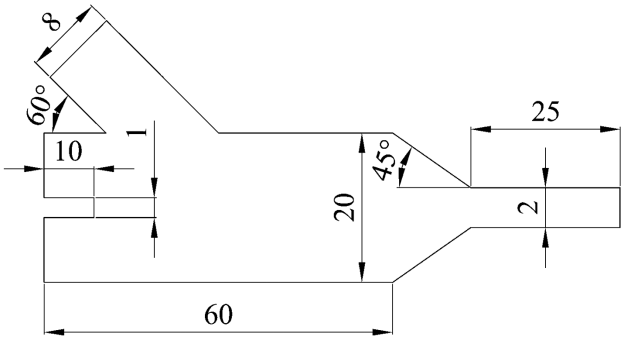


**Figure 2:** Internal cavity structure of a nozzle (mm)

### *2.3 Surface integrity characteristics*

The pickling specimen and the AWJ specimen were collectively referred to as the descaled specimens, and the surface integrity of the descaled specimens was studied. A scanning electron microscope (SEM) was used to observe the surface microscopic morphology of the descaled specimens, and energy dispersive spectroscopy (EDS) was used to determine the surface composition semi-quantitatively at a voltage setting of 20 kV and an observation distance of 10 mm. A TR200 handheld roughness meter was used to measure the surface roughness of the descaled specimens. In accordance with the requirements of GB/T 2031-2009, the measurement length $l$ was taken as 2.5 mm and the evaluation length $l_n$ was taken as 12.5 mm. The contour arithmetic mean deviation ($R_a$) and microscopic unevenness ten-point height ($R_z$) were selected to characterize the surface roughness. A Leica VMHT30M Vickers hardness tester was used to measure the cross-sectional microhardness distribution of the descaled specimens. The cross-sectional surfaces of the specimens were sanded using 400, 800 and 1500 mesh abrasive paper, and the microhardness within a depth of 2 mm from the surface was measured in three directions from the edge inwards in turn, with a measurement point interval of 0.05 mm. The measurement scheme is shown in **Figure 3**. The experimental load of 50 g was automatically loaded and held for 10 s to form a diamond-shaped indentation. The rhombic indentation was observed by a 400× optical microscope. We adjusted the knob to align the two standard lines to each vertex of the rhombic indentation and measure the microhardness of the point.

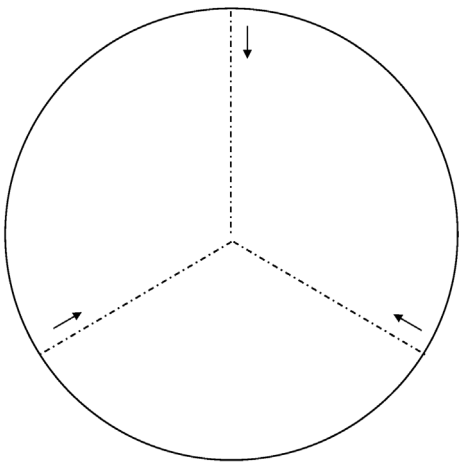

**Figure 3:** Measurement solutions for microhardness

### *2.4 Tensile test and acetic acid salt spray test (AASS)*

A WDW-200D universal testing machine was used to perform a room-temperature tensile test on the descaled specimens. During the processing of the tensile specimens in accordance with GB/T 228.1-2010, the tensile rate ($e_{Lc}$) was 0.002 $s^{-1}$, and the tensile strength ($R_m$), yield strength ($R_{p0.2}$) and elongation after fracture ($A$) of the specimens were obtained.

A YSL214-625 salt spray thermostat was used for AASS on the descaled specimens. All the reagents in the experiment were used chemically pure. The conductivity was not higher than 20 μS/cm of sodium chloride dissolved in distilled water at a temperature of 25 °C; the concentration of the sodium chloride spray solution was 50 g/L. After adding the appropriate amount of glacial acetic acid spray, the pH value of the spray solution was 3.19, and the experimental temperature was kept at 35 °C. Six descaled specimens of $\phi$ 6.5 mm × 150 mm (the pickling specimens numbered as 1# to 3#, the AWJ specimens numbered as 4# to 6#) were put into the salt spray thermostat alternatively for 48 h of AASS. They were observed every 2 h for the first 8 h of the experiment and the surface morphology was photographed and recorded. Later they were observed every 8 h between 8$^{th}$ and 48$^{th}$ hour and the surface morphology was photographed and recorded too.

## 3 RESULTS AND DISCUSSION

### *3.1 Surface integrity characteristics*

The surface morphology of an AWJ specimen observed with the SEM is shown in **Figure 4a**. Its surface is relatively flat, it appears to have a stacked organization, and there is no pressure crater. 304 stainless steel pellets of $\phi$ 0.3 mm were used to act on the 304 stainless steel wire. The abrasive was nearly spherical and strain-induced martensite was formed due to cold deformation during the use,[11] resulting in a hardness increase of the abrasive. High-speed abrasives firstly acted directly on the wire surface oxidation layer, as the oxidation layer was a brittle material, quickly broken and removed under the impact of high-speed abrasives,[12] followed by an abrasive action on the surface of the substrate poor-Cr layer. 304 stainless steel abrasives are deformable abrasives, with a slightly higher hardness than the substrate. High-speed deformable abrasives pierced into the substrate to form craters and extrude metal materials. A stack laminar characteristic was formed due to multiple deformation of multiple abrasives.

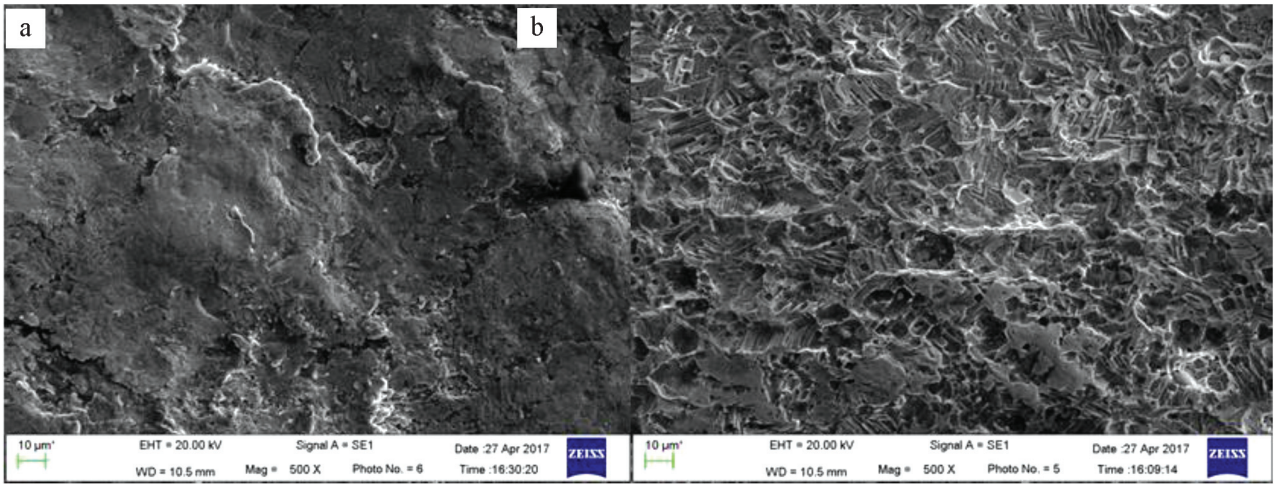


**Figure 4:** Surface morphology of descaled specimens: a) AWJ, b) pickling

The surface morphology of a pickling specimen was observed under the electron microscope as shown in **Figure 4b**. Due to the uneven corrosion of the pickling sample, etch pits of different sizes formed on the specimen surface. Acid removal of the oxide layer was carried out after further corrosion of the surface poor-Cr layer. Due to the influence of the roughness, local pitting occurred firstly, followed by a further expansion of the etch pits, removing the surface poor-Cr layer while causing corrosion of the substrate. So it is difficult to avoid a certain loss of metal caused by pickling.

The mass percentages of the main chemical elements on the surfaces of the pickling and AWJ specimens were determined semi-quantitatively with EDS as shown in **Table 2**. The mass percentages of Fe and O on the surfaces of the AWJ specimens were higher than those of the pickling specimens, and the mass percentages of Cr and Ni were lower for the AWJ specimens than for the pickling specimens. The moisture on the surface of the AWJ specimens quickly dried at the exit of the descaling box using hot air. As serious secondary oxidation occurred during the short dwell time in the high-humidity descaling box, the Cr-poor layer microstructure could easily form again on the surface layer, reducing the corrosion resistance of the material.

**Table 2:** Mass percentages ($w$/%) of the main components on the surfaces of descaled specimens

| | Fe | Cr | Ni | O |
|---|---|---|---|---|
| Pickling | 63.09 | 23.84 | 11.62 | 1.45 |
| AWJ | 71.9 | 14.25 | 10.02 | 3.83 |

The surface roughness values of the pickling specimens were $R_a$ of 4.384 µm and $R_z$ of 24.81 µm, while the values for the AWJ specimens were $R_a$ of 3.960 µm and $R_z$ of 22.63 µm. The surface roughness of the pickling specimens was slightly higher than that of the AWJ specimens. The surface roughness of the pickling specimens was determined by the etch pits of different sizes, and it also related to the roughness of the original specimen. The surface of the AWJ specimens exhibited a lower roughness of the stack laminar characteristic. The surface roughness was mainly determined by the jet pressure, combined with the abrasive and target material.

The microhardness of the descaled specimens changed in three depth directions as shown in **Figure 5**. The microhardness of the pickling specimens was fluctuating. The microhardness was basically in a range of 200–220 HV. The microhardness of 304 stainless steel was less than 200 HV, the experimental material was a wire of $\phi$ 6.5 mm. After plastic deformation, the material hardness increased, indicating that the pickling process did not affect the microhardness of 304 stainless steel. The microhardness of the AWJ specimens decreased with the increase in the distance from the surface. In a range of 0–0.3 mm from the surface, it decreased rapidly from 390 HV to 240 HV. In a range of 0.3–1.0 mm from the surface, it decreased slowly from 240 HV to 210 HV, and in a range of 1.0–2.0 mm from the surface, it fluctuated slightly less than in the case of pickling and descaling at the same distance.

Chen et al.[13] found a similar pattern of surface-microhardness changes in a study of stress shot peening of 2205 stainless steel. As a high-speed abrasive continuously hit the surface of a specimen, part of the kinetic energy of the abrasive was absorbed by the specimen and plastic deformation occurred on its surface. The surface microhardness increased from the original 210 HV to 380–390 HV, corresponding to the change in the surface hardness of a compressed specimen with 60–80 % deformation. It produced a work-hardening layer of about 1 mm in depth, which had a large impact on the substrate 0–0.3 mm from the surface. The jet of the nozzle covered a certain curved surface of the material. The distance from the nozzle to the centre of the curved surface and the boundary varied slightly. So the microhardness of the AWJ specimens changed in the three depth directions

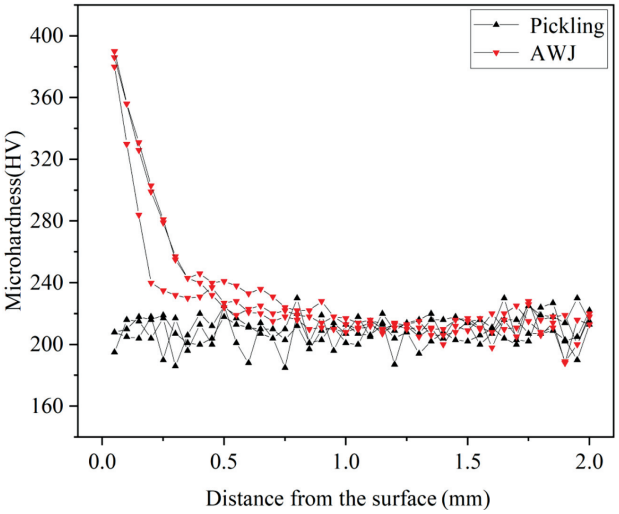


**Figure 5:** Changes in the microhardness of descaled specimens

measured as roughly the same pattern, but there were differences.

AWJ introduces a residual stress field on the surface layer of the material, causing a refinement of the tissue and strain-induced martensite formation. All these changes have an impact on the surface hardness of the material, specifically:[14–16]

1) When subjected to a residual compressive stress, the microhardness increases and the indentation produced by the indenter during the microhardness measurement is smaller.

2) The process of abrasive water jetting causes a plastic flow in the surface metal and a reduction in the grain size. According to the Hall-Petch formula, the smaller the size of the grain, the higher is the strength of the material. The higher the density of defects such as dislocations, grain boundaries and layer errors, the greater is the resistance to dislocation movement and the harder is the material.

3) Under the effect of AWJ, strain-induced martensite forms on the surface layer. Martensite has a high strength due to the hard phase in the material. It can impede the dislocation movement and strengthen the matrix.

### *3.2 Tensile test and acetic acid salt spray test*

#### *3.2.1 Tensile test*

The tensile properties of three sets of descaled specimens under room temperature are shown in **Table 3**. The yield strength and tensile strength of the pickling specimens were slightly increased. The elongation after fracture was significantly lower compared to the AWJ specimens. Both hydrogen embrittlement caused by pickling and work hardening caused by AWJ resulted in an increase in the strength and a decrease in the plasticity.[17,18] Comparing the two processes, hydrogen embrittlement had a greater effect on the mechanical properties of the material. The elongation after fracture of the pickling specimens was 12.5 % lower than that of the AWJ specimens, resulting in a more severe reduction in the cold formability of the material.

**Table 3:** Tensile properties of descaled specimens under room temperature

| | Yield strength (MPa) | | | Tensile strength (MPa) | | | Elongation after fracture (%) | | |
|---|---|---|---|---|---|---|---|---|---|
| Pickling | 311 | 332 | 340 | 611 | 625 | 630 | 61.2 | 58.39 | 58.8 |
| AWJ | 289 | 313 | 282 | 599 | 591 | 592 | 74.8 | 70 | 71.2 |

#### *3.2.2 Acetic acid salt spray test (AASS)*

The pickling specimens were marked as 1# to 3#, having a white surface and metallic luster, and the AWJ specimens were marked as 4# to 6#, having an opaque surface and inconspicuous metallic luster, as shown in **Figure 6**. The surface oxidation of the AWJ specimens was higher than that of the pickling specimens, so the surface was opaque, losing its metallic luster. The pickling specimens did not show any rust spots on the surface during the 48 h of AASS and remained white and bright with a metallic luster. As the AASS test was carried out for 2 h, yellow-brown rust spots appeared on the surface of the AWJ specimens, and they grew on the surface of the samples during the AASS test from 2$^{nd}$ to 48$^{th}$ hour. The surface rust spots after 24 h are shown in **Figure 7**.

The surface rust spots covered more than 80 % of the surface after 48 h of the AASS test. The surface conditions of the pickling specimen and the AWJ specimen after the 48 h of the AASS experiment are shown in **Figure 8**. The corrosion resistance of the pickling specimens was significantly better than that of the AWJ specimens. Wang et al.[19] studied sandblasted 304 stainless steel and

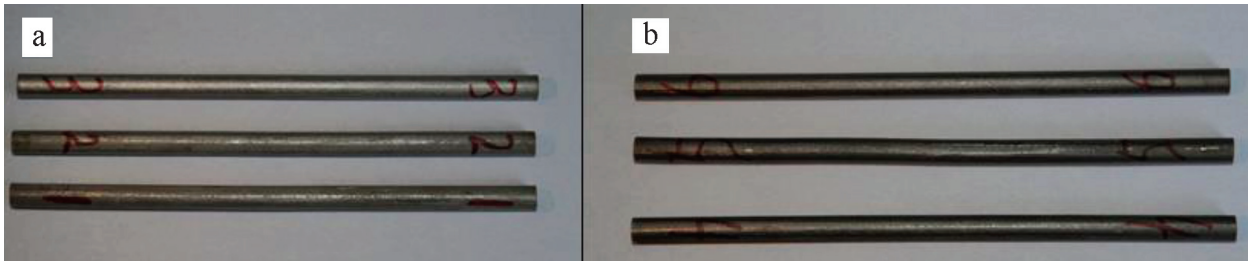


**Figure 6:** Surface conditions of the specimens before the start of AASS: a) pickling, b) AWJ


**Figure 7:** Surface of AWJ specimen No. 5 after 24 h of AASS

found that the surface was significantly enhanced by the formation of a nanocrystalline surface layer after sandblasting, but the corrosion resistance was significantly reduced compared with that of the original specimens. With regard to roughness, the surface roughness of the pickling specimens was greater and was more likely to cause surface pore corrosion. With regard to residual stress, the surface layer of the AWJ specimens produced a residual compressive stress field, reducing stress corrosion and improving corrosion resistance.

However, the secondary oxidation of the surface layer of the AWJ specimens was serious. The surface layer generated a Cr-poor layer with a Cr content below 12 %; so the stainless steel lost its excellent corrosion resistance also due to the depletion of Cr. The activation of the Cr-poor zone and the passivation of the Cr-rich zone constituted an activation-passivation corrosion cell, which developed along the grain boundaries, to the point of a complete destruction of intergranular bonds. Therefore, necessary passivation is required to avoid or reduce the occurrence of secondary oxidation when the AWJ process is used to remove the scales.

## 4 CONCLUSIONS

1) The surfaces of the pickling specimens formed pits of different sizes due to uneven corrosion; $R_a$ was 4.384 μm and $R_z$ was 24.81 μm, the microhardness was fluctuating, and the microhardness value was basically in a range of 200–220 HV. The surfaces of the AWJ specimens exhibited a stack laminar characteristic; $R_a$ was 3.960 μm and $R_z$ was 22.63 μm, while the microhardness decreased with the increase in the distance from the surface. The surface microhardness increased from the original 210 HV to 380–390 HV. It produced a work hardening layer of about 1 mm in depth, which had a large effect on the substrate 0–0.3 mm from the surface.

2) The yield strength and tensile strength of the pickling specimens were slightly increased and the elongation after fracture was significantly reduced compared with the AWJ specimens. The effect of the pickling hydrogen embrittlement on the mechanical properties of the material was greater, and the elongation after fracture of the pickling specimens was 12.5 % lower than that of the AWJ specimens, leading to a more serious reduction in the cold formability of the material.

3) The corrosion resistance of the pickling specimens was significantly better than that of the AWJ specimens. In terms of roughness and residual stress, the AWJ specimens had better resistance to pitting and stress corrosion. However, due to severe secondary oxidation, the surface layer of the AWJ specimens generated a Cr-poor layer. The corrosion resistance of the material was thus reduced.

## 5 REFERENCES

[1] X. Lan, B. Hu, S. F. Wang, W. T. Luo, P. Fu, Magnetic characteristics and mechanism of 304 austenitic stainless steel under fatigue loading, Eng. Failure Anal., 136 (**2022**), 1–10, doi:10.1016/j.engfailanal.2022.106182

[2] X. W. Liao, H. L. Wei, L. Y. Feng, H. Y. Ban, Low-cycle fatigue behavior for stainless-clad 304+Q235B bimetallic steel, Int. J. Fatigue, 159 (**2022**), 1–12, doi:10.1016/j.ijfatigue.2022.106831

[3] S. Kossman, L. B. Coelho, A. Mejias, A. Montagne, A. Van Gorp, T. Coorevits, M. Touzin, M. Poorteman, M.-G. Olivier, A. Iost, M. H. Staia, Impact of industrially applied surface finishing processes on tribocorrosion performance of 316L stainless steel, Wear, 456–457 (**2020**), 1–14, doi:10.1016/j.wear.2020.203341

[4] X. H. Chen, J. Lu, L. Lu, K. Lu, Tensile properties of a nanocrystalline 316L austenitic stainless steel, Scr. Mater., 52 (**2005**) 10, 1039–1044, doi:10.1016/j.scriptamat.2005.01.023

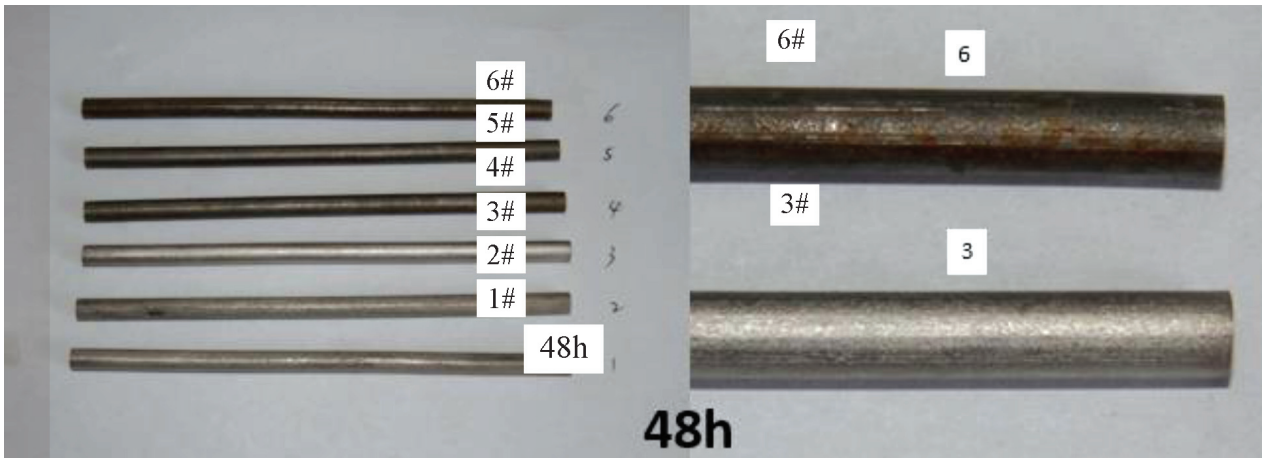


**Figure 8:** Surface conditions of specimens after 48h of AASS: a) pickling specimens (No. 1 to No. 3) and AWJ specimens (No. 4 to No. 6), b) local enlargement of specimens No. 3 and No. 6

[5] S. N. Geng, J. S. Sun, L. Y. Guo, Effect of sandblasting and subsequent acid pickling and passivation on the microstructure and corrosion behavior of 316L stainless steel, Mater. Des., 8 (**2015**), 1–7, doi:10.1016/j.matdes.2015.08.113

[6] E. Tcharkhtchi-Gillard, M. Benoit, P. Clavier, B. Gwinner, F. Miserque, V. Vivier, Kinetics of the oxidation of stainless steel in hot and concentrated nitric acid in the passive and transpassive domains, Corros. Sci., 107 (**2016**), 182–192, doi:10.1016/j.corsci.2016.02.031

[7] X. B. Li, M. Gao, H. Z. Li, W. W. Xing, Z. Long, S. Lei, Z. Xiujuan, M. Yingche, L. Kui, Effect of residual hydrogen content on the tensile properties and crack propagation behavior of a type 316 stainless steel, Int. J. Hydrogen Energy, 44 (**2019**), 25054–25063, doi:10.1016/j.ijhydene.2019.07.131

[8] Y. Natarajan, P. K. Murugesan, M. Mohan, S. A. L. A. Khan, Abrasive Water Jet Machining Process: A state of art of review, Journal of Manufacturing Processes, 49 (**2020**), 271–322, doi:10.1016/j.jmapro.2019.11.030

[9] K. Balaji, M. S. Kumar, N. Yuvaraj, Multi objective taguchi–grey relational analysis and krill herd algorithm approaches to investigate the parametric optimization in abrasive water jet drilling of stainless steel, Applied Soft Computing Journal, 102 (**2021**), 1–25, doi:10.1016//j.asoc.2020.107075

[10] W. X. Wang, Z. J. Zheng, C. Y. Zhou, Effect of heat treatment on the mechanical properties of surface shot blasted nanocrystalline 304 stainless steel, Heat Treatment of Metal, 43 (**2018**) 11, 84–88, doi:10.13251/j.issn.0254-6051.2018.11.019

[11] N. Na, H. B. Wu, J. M. Cao, G. Niu, L. X. Xu, Effect of cold deformation on the organization and properties of 304 austenitic stainless steel, Hot Working Technology, 47 (**2018**) 4, 62–66, doi:10.14158/j.cnki.1001-3814.2018.04.015

[12] Y. Guo, F. Q. Dai, S. T. Hu ,Y. Gao, Effect of Annealing Time on Oxides Phases and Morphology along Oxidized Depth of Fe-3%Si Steel during Decarburization, ISIJ Int., 59 (**2019**) 1, 152–160, doi:10.2355/isijinternational.isijint-2018-441

[13] M. Chen, C. H. Jiang, Z. Xu, V. Ji, Surface layer characteristics of SAF2507 duplex stainless steel treated by stress shot peening, Appl. Surf. Sci., 481 (**2019**), 226–233, doi:10.1016/j.apsusc.2019.03.045

[14] Y. Sun, D. Zhang, L. J. Wu, Q. M. Wang, Analysis of the degree of influence of material residual stress on hardness testing, Journal of East China University of Science and Technology (Natural Science Edition), 38 (**2012**) 5, 652–656, doi:10.14135/j.cnki.1006-3080.2012.05.022

[15] S. Carlsson, P. L. Larsson, On the determination of residual stress and strain fields by sharp indentation testing. Part II: experimental investigation, Acta Mater., 42 (**2001**) 12, 2193–2203, doi:10.1016/S1359-6454(01)00123-9

[16] J. P. Nobre, A. M. Dias, M. Kornmeier, An empirical methodology to estimate a local yield stress in work-hardened surface layers, Society for Experimental Mechanics, 44 (**2004**) 1, 76–84, doi:10.1007/BF02427980

[17] T. Wang, H. Y. Zhang, W Liang, Hydrogen embrittlement fracture mechanism of 430 ferritic stainless steel: The significant role of carbides and dislocations, J. Mater. Sci. Eng. A, 829 (**2022**), 1–13, doi:10.1016/j.msea.2021.142043

[18] Y. H. Fan, B. Zhang, J. Q. Wang, E.-H. Han, W. Ke, Effect of grain refinement on the hydrogen embrittlement of 304 austenitic stainless steel, J. Mater. Sci. Technol., 35 (**2019**) 10, 2213–2219, doi:10.1016/j.jmst.2019.03.043

[19] X. Y. Wang, D. Y. Li, Mechanical and electrochemical behavior of nanocrystalline surface of 304 stainless steel, Electrochim. Acta, 47 (**2002**), 3939–3947, doi:10.1016/S0013-4686(02)00365-1